

# CHEMISTRY

---

## AN **ASIAN** JOURNAL

[www.chemasianj.org](http://www.chemasianj.org)



A Journal of



# REPRINT

WILEY-VCH

## Graphene Quantum Dots

## Covalent Crosslinking of Graphene Quantum Dots by McMurry Deoxygenation Coupling

Limei Chen, Peiguang Hu, Jia En Lu, and Shaowei Chen<sup>\*[a]</sup>

**Abstract:** Graphene quantum dots were covalently cross-linked forming ensembles of a few hundred nanometers in size by McMurry deoxygenation coupling reactions of peripheral carbonyl functional moieties catalyzed by TiCl<sub>4</sub> and Zn powders in refluxing THF, as evidenced by TEM, AFM, FTIR, Raman and XPS measurements. Photoluminescence measurements showed that after chemical coupling, the excitation and emission peaks blue-shifted somewhat and the emission intensity increased markedly, likely due to the removal of oxygenated species where quinone-like species are known to be effective electron acceptors and emission quenchers.

Graphene oxide (GO) nanosheets have been attracting extensive research interest due to their unique optical and electronic properties and potential applications in diverse areas such as optoelectronics, catalysis, energy generation and storage.<sup>[1]</sup> GO is generally prepared by chemical (oxidative) exfoliation of bulk graphite and carries a number of oxygenated functional groups such as carboxyl, carbonyl, hydroxyl, etc.<sup>[1c]</sup> which render GO readily dispersible in water and polar organic media and may be exploited for the anchored deposition of metal and metal oxide nanoparticles forming functional nanocomposites.<sup>[2]</sup> Towards this end, it is critical to develop effective procedures for the controlled, “bottom-up” assembly of graphene derivatives into large, complicated architectures. In fact, ensembles of GO nanosheets have been prepared by employing molecular or metal templates, interfacial condensation driven by solvent evaporation at separated phases, and Langmuir-based techniques.<sup>[3]</sup> For instance, DNA molecules have been used for the controlled assembly of GO, and 3D GO networks have been formed on the metal surfaces (Zn, Fe, Cu, etc.) by a substrate-assisted reduction and assembly method.<sup>[3a, d]</sup> GO thin films have also been prepared at the dimethyl formamide/air interface, while a honeycomb film is formed on a glass slide

by the self-assembly of dimethyldioctadecylammonium bromide-modified GO.<sup>[3b, 4]</sup> Large transparent conducting films have also been produced by Langmuir–Blodgett assembly of small graphene sheets in a layer-by-layer manner.<sup>[3c]</sup> In these earlier studies, GO nanosheets were assembled into different architectures mostly through noncovalent interactions such as electrostatic or van der Waals interactions. One immediate question arises. Is it possible to covalently crosslink GO nanosheets such that mechanically robust ensembles may be produced? This is the primary motivation of the present study, where controlled assembly of graphene quantum dots (GQDs) is achieved by exploiting the unique chemical reactivity of the GQD peripheral oxygenated species.<sup>[5]</sup> Specifically, GQDs are covalently crosslinked by C=C bonds formed by McMurry deoxygenation coupling of the GQD peripheral carbonyl groups.<sup>[6]</sup>

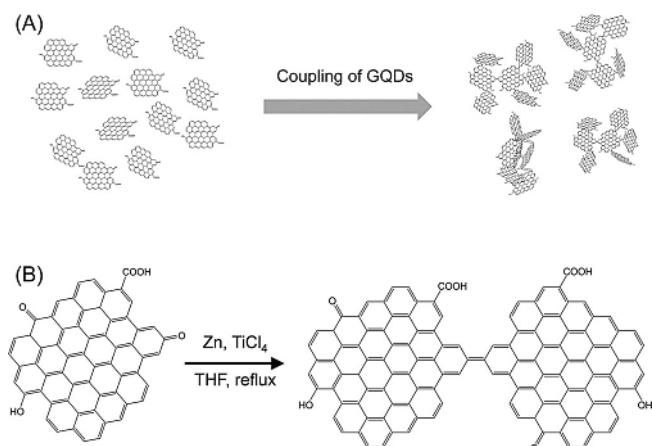
In the McMurry reaction, aldehydes and ketones are reduced by low-valence titanium compounds in THF or 1,4-dioxane to afford pinacols and/or olefins in high yields; and refluxing at elevated temperatures leads to effective deoxygenation of the reactant molecules to produce olefins (up to 98% yield).<sup>[7]</sup> For instance, two 2-methyl-2,3-dihydro-1*H*-cyclopenta[*a*]naphthalen-1-one molecules have been coupled to produce the corresponding alkene by thermal refluxing in THF in the presence of TiCl<sub>4</sub> and Zn powders.<sup>[8]</sup>

Notably, GQDs prepared by acid exfoliation of graphite precursors are rich of oxygen-containing functional groups at the surfaces and edges,<sup>[1c]</sup> where the carbonyl groups may be exploited as the active sites for McMurry coupling between GQDs. Herein, 3D networks of GQDs were obtained via covalent coupling by thermal refluxing in THF with TiCl<sub>4</sub> and Zn powders as the catalysts (Scheme 1). The structures of the resulting GQD ensembles were carefully examined by various microscopic and spectroscopic measurements.

Experimentally, GQDs were prepared by acid exfoliation of the nanometer-sized sp<sup>2</sup> domains in pitch carbon fibers (see the Supporting Information for details).<sup>[1c]</sup> The obtained GQDs were decorated with various oxygenated species, such as epoxy and carbonyl groups, and are readily dispersible in water and polar organic media (Figure S1).<sup>[9]</sup> Figure 1A depicts a representative TEM image of the as-prepared GQDs, where individual GQDs can be easily recognized, consistent with the good dispersity of the GQDs in water. Statistical analysis based on more than 100 GQDs showed that the GQDs exhibited a narrow size distribution, with the majority of the GQDs within the size range of 3.0 to 5.0 nm and an average diameter

[a] L. Chen, Dr. P. Hu, J. E. Lu, Prof. Dr. S. Chen  
Department of Chemistry and Biochemistry  
University of California  
1156 High Street, Santa Cruz, California 95064 (USA)  
E-mail: shaowei@ucsc.edu

Supporting information and the ORCID identification number(s) for the author(s) of this article can be found under <https://doi.org/10.1002/asia.201700225>.



**Scheme 1.** Schematic of (A) covalent crosslinking of GQDs by (B) McMurry deoxygenation coupling reaction.

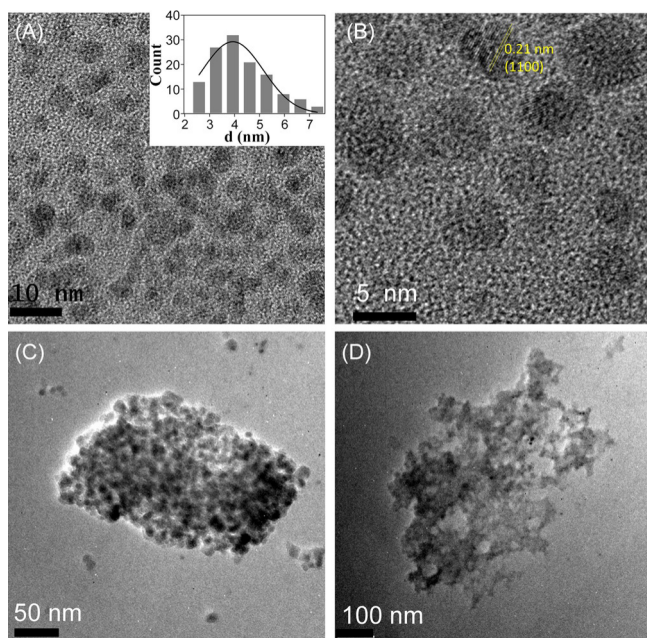


**Figure 1.** (A) TEM images of GQDs as synthesized from carbon fibers. Inset: size distribution of GQDs. (B) HRTEM of GQDs. TEM images of (C) GQDs-CL and (D) GQDs-CH.

of  $4.3 \pm 1.2$  nm, as depicted in the inset. Figure 1B shows the corresponding high-resolution TEM image where well-defined lattice fringes can be seen with a lattice spacing of 0.21 nm, in good agreement with the interplanar distance of carbon (1100).<sup>[10]</sup>

Remarkably, after McMurry deoxygenation coupling catalyzed by  $\text{TiCl}_4$  and zinc in refluxing THF,<sup>[6–8]</sup> significant crosslinking of GQDs occurred. Two samples were prepared, GQDs-CH and GQDs-CL, where the amount of  $\text{TiCl}_4$  and zinc added was twice as much in the former as in the latter (see the Supporting Information for details). Both samples remained dispersible in water, but barely in THF. From Figure 1C, one can see that the GQDs-CL sample exhibited the formation of ensembles up

to 300 nm across, and even larger agglomerates can be found with the GQDs-CH sample (ca. 600 nm in size, Figure 1D). These observations suggest effective covalent crosslinking of GQDs by the McMurry deoxygenation coupling reaction (Scheme 1A).<sup>[1c]</sup> In this reaction,  $\text{Ti}^{\text{IV}}$  was reduced by metallic Zn to produce low-valence titanium ( $\text{Ti}^{\text{II}}$  or  $\text{Ti}^{\text{III}}$ ) which served as catalysts to facilitate the deoxygenation of the GQD carbonyl groups and subsequent covalent coupling between the GQDs (Scheme 1B).

AFM and dynamic light scattering (DLS) measurements further confirmed the coupling of GQDs by McMurry deoxygenation. Figure 2 depicts the representative AFM topographs of the (A<sub>1</sub>) as-prepared GQDs, (B<sub>1</sub>) GQDs-CL, and (C<sub>1</sub>) GQDs-CH, where individual GQDs and crosslinked ensembles can be readily resolved. Again, this is consistent with the good dispersity of the samples in water. The corresponding line scan profiles were included in panels (A<sub>2</sub>), (B<sub>2</sub>), and (C<sub>2</sub>). One can see that the thickness of the samples increased markedly in the order of as-prepared GQDs < GQDs-CL < GQDs-CH. In fact, from the height histogram (Figure 2A<sub>3</sub>), the height of the as-prepared GQDs was mostly in the range of 0.6 to 1.2 nm, with an average of  $1.0 \pm 0.4$  nm, corresponding to 1 to 4 graphene layers.<sup>[1c]</sup> In contrast, the heights of both GQDs-CL and GQDs-CH were markedly greater at  $5.0 \pm 2.8$  nm (Figure 2B<sub>3</sub>) and  $17.2 \pm 10.5$  nm (Figure 2C<sub>3</sub>), respectively. That is, with the addition of an increasing amount of coupling reagents, the size of the GQD ensembles increased accordingly, consistent with the TEM results in Figure 1. A similar variation was observed in DLS measurements, where the average hydrodynamic radius ( $R_{\text{H}}$ ) in water of the as-prepared GQDs was estimated to be 20.7 nm, which increased drastically to 57.8 nm for GQDs-CL and 237.2 nm for GQDs-CH.

The chemical structures of the GQDs before and after McMurry coupling were further examined by FTIR measurements. From Figure S2, one can see that the as-prepared GQDs (black curve) exhibited multiple characteristic peaks at  $3428 \text{ cm}^{-1}$  (O–H stretch),  $1738 \text{ cm}^{-1}$  (C=O stretch),  $1620 \text{ cm}^{-1}$  (aromatic C=C stretch),  $1405 \text{ cm}^{-1}$  (symmetrical stretch of O–H in COOH), and  $1197$  and  $1046 \text{ cm}^{-1}$  (C–O–C vibrations).<sup>[11]</sup> This strongly indicates the formation of oxygen-containing functional groups such as hydroxyl, carbonyl, carboxyl and epoxy groups in GQDs.<sup>[11a]</sup> After deoxygenation coupling, whereas these vibrational bands remained visible, the intensity of the oxygenated moieties decreased significantly with respect to that of the C=C vibration. For instance, the relative intensity of the C=O vibrational band at  $1738 \text{ cm}^{-1}$  to that of aromatic C=C vibration at  $1620 \text{ cm}^{-1}$  was reduced by 40% for GQDs-CL and 74% for GQDs-CH, as compared to that of the as-prepared GQDs. This is consistent with the effective removal of the C=O groups in McMurry deoxygenation coupling which was facilitated by increasing loading of the coupling catalysts.

More quantitative analysis was carried out with XPS measurements. From the survey spectra in Figure S3, one can see that the as-prepared GQDs, GQDs-CL and GQDs-CH samples all exhibited only two major peaks at around 285 and 532 eV, corresponding to the binding energies of C 1s and O 1s electrons, respectively. The high-resolution scans of the C 1s electrons

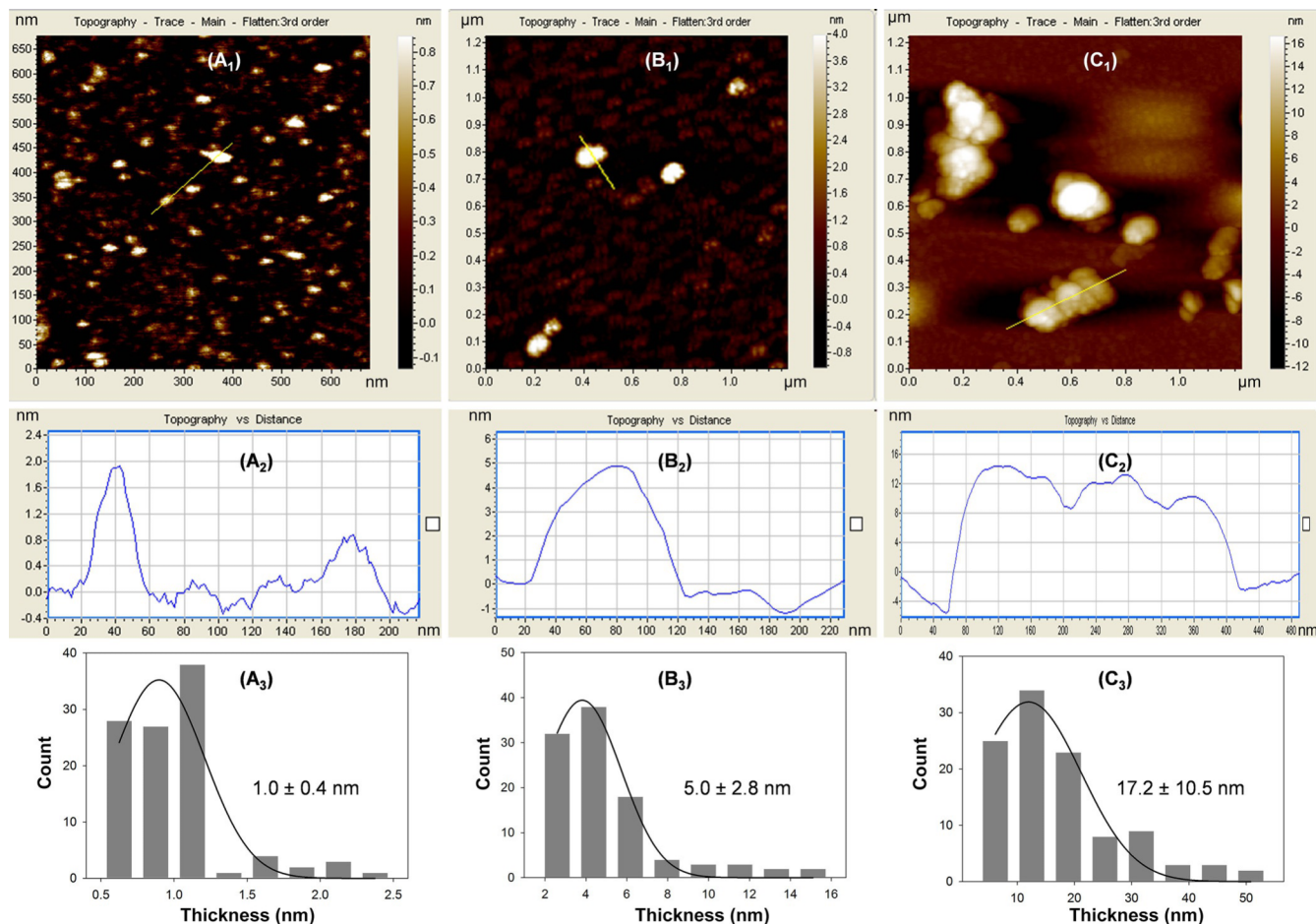


**Figure 2.** Representative AFM topographs, line scans and height distributions of (A<sub>1</sub>–A<sub>3</sub>) GQDs, (B<sub>1</sub>–B<sub>3</sub>) GQDs-CL, and (C<sub>1</sub>–C<sub>3</sub>) GQDs-CH.

are depicted in Figure 3. From Figure 3A, it can be seen that the C 1s spectrum of the as-prepared GQDs can be deconvoluted into three subpeaks at 284.5 eV, 285.5 eV, and 287.7 eV, which may be assigned to sp<sup>2</sup>-hybridized carbon (C=C), sp<sup>3</sup>-hybridized C (C–O) and carbon in C=O, respectively.<sup>[12]</sup> This indicates that the GQDs were indeed functionalized with a number of oxygenated species, as suggested by FTIR measurements (Figure S2). For the GQDs-CL (Figure 3B) and GQDs-CH (Figure 3C) samples, deconvolution of the C 1s spectra also yielded three subpeaks at similar binding energies. However, the concentration of the oxidized carbon (C=O) varied markedly from GQDs to GQDs-CL and GQDs-CH, based on the integrated peak areas. For instance, C=O accounted for 15.3% of the carbon atoms in the as-prepared GQDs, but only 9.8% in GQDs-CL and 6.2% in GQDs-CH; and concurrently, the fraction of sp<sup>2</sup> C increased from 61.3% in GQDs to 64.3% in GQDs-CL and 71.9% in GQDs-CH (whereas the contents of sp<sup>3</sup> carbons remained almost invariant at 23.5% for GQDs, 25.8% for GQDs-CL, and 21.8% for GQDs-CH). Moreover, the C:O mole ratio increased from 6.5 for as-prepared GQDs to 10.2 for GQDs-CL and 16.1 for GQDs-CH. These results are highly consistent with McMurry deoxygenation of the carbonyl moieties and the subsequent formation of C=C covalent linkages that crosslinked GQDs.<sup>[8]</sup>

Consistent results were obtained in Raman measurements. As shown in Figure S4, the three GQDs samples all exhibited a D band at 1351 cm<sup>-1</sup> and a G band at 1578 cm<sup>-1</sup>,<sup>[11a,12,13]</sup> and the ratio of the two band intensities ( $I_D/I_G$ ) was found to decrease from 1.44 for GQDs to 1.26 for GQDs-CL and 0.94 for GQDs-CH, due to the removal of the oxidized carbons (defects) from the GQD molecular skeletons.

Interestingly, the photoluminescence properties of the GQDs also varied after chemical coupling. For instance, as depicted in Figure 4, whereas both the as-produced GQDs and GQDs-CL exhibited a major excitation peak ( $\lambda_{ex}$ ) at 368 nm and a corresponding emission peak ( $\lambda_{em}$ ) at 550 nm,  $\lambda_{ex}$  and  $\lambda_{em}$  blue-shifted to 360 and 518 nm, respectively, for GQDs-CH. In addition, the photoluminescence intensity (normalized to respective absorbance at the excitation wavelength, Figure S5) was markedly enhanced with GQDs-CH as compared to those of as-produced GQDs and GQDs-CL. This, again, is consistent with the removal of oxygenated species on the GQD surface where quinone-like species are known to be effective electron acceptors and emission quenchers.<sup>[14]</sup> A similar blue-shift of the peak position of photoluminescence emission and enhanced emission intensity has also been observed with GQDs reduced by sodium borohydride, which is ascribed to the removal of carbonyl and epoxy groups from the GQD surface.<sup>[11a,15]</sup>

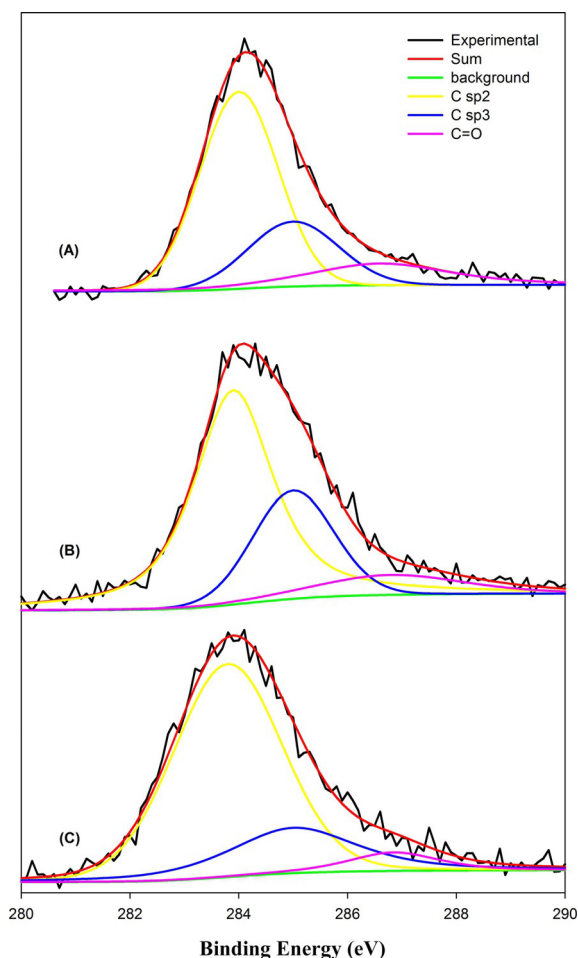


**Figure 3.** High-resolution XPS scans of the C 1s electrons in (A) as-prepared GQDs, (B) GQDs-CL, and (C) GQDs-CH. Black curves are experimental data and colored curves are deconvolution fits.

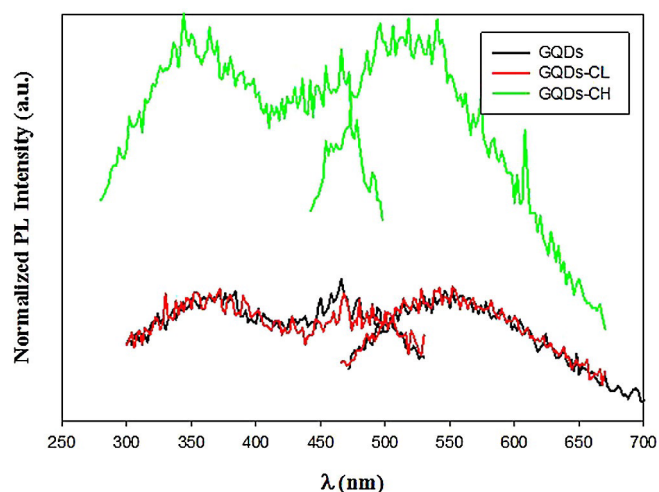


**Figure 4.** Excitation and emission spectra of as-produced GQDs, GQDs-CL, and GQDs-CH in water. The photoluminescence intensity has been normalized to the respective absorbance (Figure S5) at the excitation position.

In summary, a facile method was developed to covalently crosslink small GQDs of less than 10 nm into large superstruc-

tures of hundreds of nanometers in size by taking advantage of the McMurry deoxygenation reaction for the conversion of ketones or aldehydes to olefins. Specifically, GQDs prepared by acid exfoliation of carbon fibers were readily dispersed both in water and THF, and the peripheral carbonyl moieties provide the active sites for GQD covalent crosslinking catalyzed by  $\text{TiCl}_4$  and Zn, as manifested in various microscopic and spectroscopic measurements. The results may be exploited as a generic, effective strategy for controllable assembly of graphene oxide and derivatives into more complicated functional architectures.

### Acknowledgements

This work was supported in part by the US National Science Foundation (DMR-1409396). TEM and XPS work was carried out at the National Center for Electron Microscopy and Molecular Foundry, respectively, at the Lawrence Berkeley National Laboratory, which is supported by the US Department of Energy, as part of a user project.

### Conflict of interest

The authors declare no conflict of interest.

**Keywords:** covalent crosslinking · graphene quantum dots · McMurry deoxygenation coupling · oxygenated moiety · photoluminescence

- [1] a) T. Yoon, J. H. Kim, J. H. Choi, D. Y. Jung, I. J. Park, S. Y. Choi, N. S. Cho, J. I. Lee, Y. D. Kwon, S. Cho, T. S. Kim, *ACS Nano* **2016**, *10*, 1539–1545; b) K. S. Novoselov, V. I. Fal'ko, L. Colombo, P. R. Gellert, M. G. Schwab, K. Kim, *Nature* **2012**, *490*, 192–200; c) J. Peng, W. Gao, B. K. Gupta, Z. Liu, R. Romero-Aburto, L. H. Ge, L. Song, L. B. Alemany, X. B. Zhan, G. H. Gao, S. A. Vithayathil, B. A. Kaiparettu, A. A. Marti, T. Hayashi, J. J. Zhu, P. M. Ajayan, *Nano Lett.* **2012**, *12*, 844–849; d) J. Wen, Y. Q. Xu, H. J. Li, A. P. Lu, S. G. Sun, *Chem. Commun.* **2015**, *51*, 11346–11358; e) F. H. Li, S. Y. Gan, D. X. Han, L. Niu, *Electroanalysis* **2015**, *27*, 2098–2115.
- [2] a) Y. Song, S. W. Chen, *ACS Appl. Mater. Interfaces* **2014**, *6*, 14050–14060; b) D. Y. Pan, J. K. Jiao, Z. Li, Y. T. Guo, C. Q. Feng, Y. Liu, L. Wang, M. H. Wu, *ACS Sustainable Chem. Eng.* **2015**, *3*, 2405–2413.
- [3] a) L. H. Tang, Y. Wang, Y. Liu, J. H. Li, *ACS Nano* **2011**, *5*, 3817–3822; b) Y. F. Bai, Y. F. Zhang, A. W. Zhou, H. W. Li, Y. Zhang, J. H. T. Luong, H. F. Cui, *Nanotechnology* **2014**, *25*, 405601; c) X. L. Li, G. Y. Zhang, X. D. Bai, X. M. Sun, X. R. Wang, E. Wang, H. J. Dai, *Nat Nanotechnol* **2008**, *3*, 538–542; d) C. G. Hu, X. Q. Zhai, L. L. Liu, Y. Zhao, L. Jiang, L. T. Qu, *Sci. Rep.* **2013**, *3*, 2065; e) M. Ardinì, G. Golia, P. Passaretti, A. Cimini, G. Pitari, F. Giansanti, L. Di Leandro, L. Ottaviano, F. Perrozzi, S. Santucci, V. Morandi, L. Ortolani, M. Christian, E. Treossi, V. Palermo, F. Angelucci, R. Ippoliti, *Nanoscale* **2016**, *8*, 6739–6753; f) M. Q. Zeng, L. X. Wang, J. X. Liu, T. Zhang, H. F. Xue, Y. Xiao, Z. H. Qin, L. Fu, *J. Am. Chem. Soc.* **2016**, *138*, 7812–7815.
- [4] S. Y. Yin, Y. Y. Zhang, J. H. Kong, C. J. Zou, C. M. Li, X. H. Lu, J. Ma, F. Y. C. Boey, X. D. Chen, *ACS Nano* **2011**, *5*, 3831–3838.
- [5] V. Georgakilas, M. Otyepka, A. B. Bourlinos, V. Chandra, N. Kim, K. C. Kemp, P. Hobza, R. Zboril, K. S. Kim, *Chem. Rev.* **2012**, *112*, 6156–6214.
- [6] J. E. McMurry, M. P. Fleming, *J. Am. Chem. Soc.* **1974**, *96*, 4708–4709.
- [7] T. Mukaiyama, T. Sato, J. Hanna, *Chem. Lett.* **1973**, *2*, 1041–1044.
- [8] M. K. J. ter Wiel, R. A. van Delden, A. Meetsma, B. L. Feringa, *J. Am. Chem. Soc.* **2003**, *125*, 15076–15086.
- [9] Z. Y. Li, W. H. Zhang, Y. Luo, J. L. Yang, J. G. Hou, *J. Am. Chem. Soc.* **2009**, *131*, 6320–6321.

- [10] A. Ananthanarayanan, X. W. Wang, P. Routh, B. Sana, S. Lim, D. H. Kim, K. H. Lim, J. Li, P. Chen, *Adv Funct Mater* **2014**, *24*, 3021–3026.
- [11] a) W. K. Zhang, Y. Q. Liu, X. R. Meng, T. Ding, Y. Q. Xu, H. Xu, Y. R. Ren, B. Y. Liu, J. J. Huang, J. H. Yang, X. M. Fang, *Phys Chem. Chem. Phys* **2015**, *17*, 22361–22366; b) H. B. Yang, Y. Q. Dong, X. Z. Wang, S. Y. Khoo, B. Liu, *ACS Appl. Mater. Interfaces* **2014**, *6*, 1092–1099; c) O. J. Achadu, T. Nyokong, *New J. Chem.* **2016**, *40*, 8727–8736; d) L. Lin, S. Zhang, *Chem. Commun.* **2012**, *48*, 10177–10179.
- [12] D. Qu, M. Zheng, L. Zhang, H. Zhao, Z. Xie, X. Jing, R. E. Haddad, H. Fan, Z. Sun, *Sci. Rep.* **2014**, *4*, 5294.
- [13] a) L. M. Chen, P. G. Hu, C. P. Deming, N. Wang, J. E. Lu, S. W. Chen, *J Phys Chem. C* **2016**, *120*, 13303–13309; b) Z. C. Huang, Y. T. Shen, Y. Li, W. J. Zheng, Y. J. Xue, C. Q. Qin, B. Zhang, J. X. Hao, W. Feng, *Nanoscale* **2014**, *6*, 13043–13052.
- [14] L. Tian, Y. Song, X. J. Chang, S. W. Chen, *Script Mater* **2010**, *62*, 883–886.
- [15] S. J. Zhu, J. R. Shao, Y. B. Song, X. H. Zhao, J. L. Du, L. Wang, H. Y. Wang, K. Zhang, J. H. Zhang, B. Yang, *Nanoscale* **2015**, *7*, 7927–7933.

---

Manuscript received: February 14, 2017

Revised: March 21, 2017

Accepted Article published: March 22, 2017

Final Article published: April 24, 2017

---